Chemical etching of bovine serum albumin-protected Au_{25} nanoclusters for label-free and separation-free detection of cysteamine

Tong Shu, Lei Su, Jianxing Wang, Chenzhong Li, Xueji Zhang

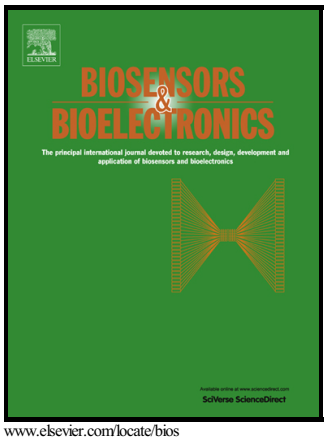

www.elsevier.com/locate/bios

PII: S0956-5663(14)00873-2
DOI: http://dx.doi.org/10.1016/j.bios.2014.10.073
Reference: BIOS7258

To appear in: *Biosensors and Bioelectronic*

Received date: 7 August 2014
Revised date: 18 October 2014
Accepted date: 31 October 2014

Cite this article as: Tong Shu, Lei Su, Jianxing Wang, Chenzhong Li and Xueji Zhang, Chemical etching of bovine serum albumin-protected Au_{25} nanoclusters for label-free and separation-free detection of cysteamine, *Biosensors and Bioelectronic,* http://dx.doi.org/10.1016/j.bios.2014.10.073

Chemical etching of bovine serum albumin-protected Au_{25} nanoclusters for label-free and separation-free detection of cysteamine

Tong Shu,[a] Lei Su,[a,*] Jianxing Wang,[a] Chenzhong Li,[b] and Xueji Zhang [a,*]

[a] Research Center for Bioengineering and Sensing Technology, Beijing Key Laboratory for Bioengineering and Sensing Technology, University of Science and Technology Beijing, Beijing 100083, P. R. China

[b] College of Engineering and Computing, Florida International University, 10555 West Flagler Street, Miami, FL 33174, USA

[*]Corresponding authors. E-mail addresses: sulei@ustb.edu.cn (L. Su); zhangxueji@ustb.edu.cn (X.J. Zhang). Tel./Fax: 86 10 8237 7347.

Abstract

This study describes a novel Au nanocluster-based fluorescent sensor for label-free, separation-free and selective detection of cysteamine (CSH). The sensing mechanism is based on CSH etching-induced fluorescence quenching of the bovine serum albumin-protected Au_{25} nanoclusters (BSAGNCs). A series of characterizations is carried out towards a better understanding of the CSH-induced fluorescence quenching of the BSAGNCs. It is found that CSH can etch the Au_{25} nanoclusters, exhibiting the potent etching activity. Other thiol-containing compounds such as glutathione and cysteine and other 19 natural amino acids do not interfere with such CSH-induced etching process. The decreases in fluorescence intensity of the

BSAGNCs allow sensitive detection of free CSH in the range of 500-10000 nM. The detection limit for CSH is 150 nM (S/N=3). The spiked human serum samples can be analyzed with satisfactory results.

Keywords: gold nanocluster; cysteamine; thiol etching; nanocluster-based biosensor; thiol sensor.

1. Introduction

Recently, the chemical etching property of thiol moieties has attracted intensive attention. For instance, thiol-induced etching is found to be extremely useful in the synthesis of metal nanoclusters (NCs) of several to hundreds of atoms (< 2 nm) (Chen et al., 2014b; Jin et al., 2010; Yu et al., 2013). Through thiol-induced etching process, the sizes of thiolated and non-thiolate-protected (e.g., surfactant and polymer) metal nanoparticles (core sizes > 2 nm) can be reduced to produce thiolated metal NCs (Chen et al., 2014b; Yu et al., 2013), and the subsequent size-focusing treatments can precisely control the size of the NCs at the atomic level (Jin et al., 2010). These synthesized metal NCs have currently become a focus of scientific research and technological innovation, due to their fascinating molecule-like properties, such as strong photoluminescence (Luo et al., 2014; Shiang et al., 2012), and their promising applications, including in catalysis (Li et al., 2014a; Li et al., 2014b), bioimaging (Shiang et al., 2012; Venkatesh et al., 2014), and biosensing (Senthamizhan et al., 2014; Su et al., 2013). Furthermore, more recently, there has been a growing interest in the thiol-induced etching of certain stable metal NCs for sensing thiols (Liu et al., 2010; Yuan et al., 2013). It has been demonstrated, for instance, that the fluorescence of lysozyme^{VI}-stabilized Au_8 NCs can be quenched through the thiol-induced etching

process, showing promising application in sensing glutathione (GSH) in biological samples (Chen and Tseng, 2012).

Thiol compounds possess a multitude of roles within physiological systems (Kruusma et al., 2006; White et al., 2002). Endogenous cysteamine (CSH) is the terminal metabolite in coenzyme A (CoA) degradation, being formed by the enzymatic cleavage of panthetheine, and also a vital source for taurine (Ueki and Stipanuk, 2009; Wu et al., 2013). CSH has many important clinical applications. For instance, CSH has been considered as a potential neuroprotective agent and exhibits significant beneficial properties in treating neurodegenerative diseases including Huntington's and Parkinson's diseases (Gibrat and Cicchetti, 2011; Mao et al., 2006; Wu et al., 2013). Also, CSH is the main drug used to treat children with nephropathic cystinosis caused by an excessive intralysosomal cystine accumulation due to a defect of its transport system in the lysosomal membrane (Kessler et al., 2008). However, because of the relatively high frequency of side effects to CSH use, some of which are dose-related, drug monitoring over the course of CSH therapy is advisable (Kusmierek et al., 2005). Thus, there is a keen interest in developing analytical methods for sensing CSH in biological samples.

Up to now, almost all strategies proposed for sensing CSH are based on the nucleophilic and reducing properties of the thiol moiety of CSH. The strong nucleophilicity of the thiol moiety of CSH is favorable for certain important reactions, for example, Michael addition reactions. Consequently, CSH has been derivatized with various optical labeling reagents, followed by high-resolution separations using chromatography and electrophoresis techniques coupled with an optical detector (Kataoka et al., 1994; Kubalczyk and Bald, 2008; Kusmierek et al., 2005; Lochman et al., 2003; Ogony et al., 2006; Stachowicz et al., 1998). On the other hand, the

reducing property of the thiol moiety enables the electroxidation of CSH at chemically modified electrodes. As a result, electrochemical methods have been used to sensitively detect CSH (Ensafi and Karimi-Maleh, 2010; Karimi-Maleh et al., 2013a; Ojani et al., 2009). For instance, CSH has been determined by high performance liquid chromatography (HPLC) for CSH separation coupled with modified electrodes for further electrochemical detection (Lochman et al., 2003; Smolin and Schneider, 1988). However, these previous methods usually need the complicated derivation procedures and/or the high-resolution separation operations.

In this study, we report for the first time a facile, label-free and separation-free method for sensitively sensing CSH. This method is based on the utilization of the chemical etching property of thiol moiety of CSH to quench the fluorescence emission of the bovine serum albumin (BSA)-protected Au_{25} NCs (BSAGNCs). BSAGNCs (Xie et al., 2009) are composed of an icosahedral Au_{13} kernel and 12 Au(I) sulphur complex, forming 6 -S-Au(I)-S-Au(I)-S- staple surface motifs (Wen et al., 2012). Eighteen thiol groups (cysteine residues) in a BSA template have been suggested to form the staple surface motifs, providing the protection of the surface atoms (Xu et al., 2014). BSAGNCs thus possess ultrastability (Xie et al., 2009), similar to other thiolated Au_{25} NCs (e.g., $Au_{25}(SG)_{18}$) (Shichibu et al., 2007). In this study, a series of characterizations was employed towards a better understanding of the mechanism of the CSH-induced fluorescence quenching of the BSAGNCs. Afterwards, a new label-free and selective fluorescent method based on the CSH-induced etching of the BSAGNCs for sensing free CSH in presence of GSH and cysteine (Cys) was established and was used to measure free CSH concentrations recovered from spiked human serum samples.

2. Experimental Section

2.1. Chemicals

L-Cysteine, L-Alanine (Ala), L-arginine (Arg), L-asparagine monohydrate (Asn), L-aspartic acid (Asp), L-glutamine (Gln), L-glutamic acid (Glu), L-glycine (Gly), L-histidine (His), L-isoleucine (Ile), L-leucine (Leu), L-lysine (Lys), L-methionine (Met), L-phenylalanine (Phe), L-proline (Pro), L-serine (Ser), L-threonine (Thr), L-tryptophan (Trp), L-tyrosine (Tyr), L-valine (Val), GSH, CSH, BSA, and $HAuCl_4 \cdot 3H_2O$ were purchased from Sigma-Aldrich. All other chemicals of at least analytical reagent were obtained from Beijing Chemical Corporation (Beijing, China). All solutions were freshly prepared with deionized water. The stock solution of the BSAGNCs was prepared according to the previous report (Xie et al., 2009).

2.2. CSH-induced etching and fluorescence quenching of the BSAGNCs

The BSAGNCs solution was incubated with 10 mM CSH at 55 ^{o}C for 1 h. Then, the resultant mixed solution was cooled at room temperature.

2.3. Effect of GSH and Cys on the fluorescence emission of the BSAGNCs

The BSAGNCs solution was incubated with 10 mM GSH and 10 mM Cys, respectively, at 55 ^{o}C for 1 h. Then, the resultant mixed solution was cooled at room temperature.

2.4. Specificity of fluorescence quenching of the BSAGNCs by CSH

Stock solutions of CSH (200 μM), GSH (200 μM), Cys (200 μM), CSH (200 μM) + GSH (200 μM), CSH (200 μM) + Cys (200 μM), and other natural amino acids (200 μ M) were freshly prepared in 5 mM phosphate buffer solution of pH 8.5 before use. 990 μL of the stock solutions was incubated separately with a solution (10 μL) of the BSAGNCs at 55 ^{o}C for 6 h. Then, the resultant mixed solutions were cooled at room

temperature, and were transferred separately into a 1 mL quartz cuvette for measuring fluorescence spectra at an excitation wavelength of 480 nm.

2.5. Determination of CSH in human serum

The calibration plot was constructed with freshly prepared phosphate buffer solutions (5 mM, pH 8.5) containing various concentrations of CSH and the resulting slope was used to calculate the concentration of CSH in human serum. Human serum was pretreated according to the previous report (Chen et al., 2012), prior to use. Briefly, 2 mL of human serum was deproteinized by adding approximately 2 mL acetonitrile and centrifuging (4000 rpm, 40 min) at room temperature. Then, acetonitrile was removed under reduced pressure on a rotary evaporator in a 60 ^{o}C water bath. The deproteinized human serum (~ 1.5 mL) was dissolved by 20 mL of 5 mM phosphate buffer solution of pH 8.5 and stored at 4 ^{o}C. A suitable volume of the diluted solution of deproteinized human serum was appropriately spiked with the standard CSH solution and three different samples with CSH at a final concentration of 6.6 μM were obtained for analysis.

2.6. Instrumentation

UV-Vis absorption spectra were recorded on a Shimadzu UV-1800 spectrometer. Fluorescence spectra of the BSAGNCs were recorded on an F-4500 spectrometer (HITACHI) at an excitation wavelength of 480 nm. X-ray photoelectron spectroscopy (XPS) spectra were recorded with a VG Scientific (United kingdom) X-ray photoelectron spectrometer (Model ESCALab220i-XL). Matrix-assisted laser desorption/ionization time-of-flight mass spectrometry (MALDI-TOF-MS) mass spectrometry was carried out on a Bruker Daltonics BIFLEX III MALDI-TOF system. Transmission electron microscopy (TEM) images were taken on a JEOL JEM-2010

microscope. All measurements were carried out at room temperature.

3. Results and discussion

3.1 Characterization of the BSAGNCs

As revealed, the as-synthesized BSAGNCs solution exhibited deep brown color under visible light (Figure 1A, item a) and emitted an intense red fluorescence under 365 nm UV light (Figure 1A, item b). The absorption peak appeared at around 520 nm (Figure 1A, black line) and the fluorescence emission peak located at 650 nm (Figure 1A, red line). These observations are consistent with previous reports (Lin et al., 2013; Su et al., 2013; Xie et al., 2009). Furthermore, the BSAGNCs solution was heated at 55^{o}C for 1 h, and then cooled down. The fluorescence emission spectrum of the BSAGNCs solution was measured at room temperature. As shown in Figure 1B, after heating at 55^{o}C for 1 h, the fluorescence emission of the BSAGNCs remained stable. Due to that the fluorescence emission of the BSAGNCs originates from the icosahedral kernel of 13 Au(0) atoms and 6 -S-Au(I)-S-Au(I)-S- semirings (Wen et al., 2012), the observed unaffected fluorescence emission indicates the thermostability of the structure of the BSAGNCs. Therefore, in the following experiments, the BSAGNCs were allowed to interact with CSH at 55^{o}C.

3.2 Fluorescence quenching of the BSAGNCs caused by the CSH-induced etching

After reacting with CSH (10 mM) at 55 ^{o}C for 1 h, the resultant solution exhibited light yellow color (Figure 1C, item a). Under 365 nm UV light, this solution emitted blue fluorescence (Figure 1C, item b). No structure in fluorescence emission spectra was observed after 600 nm (Figure 1C, blue line), indicating almost 100% quenching of the red fluorescence of the BSAGNCs by CSH. Moreover, the broad absorption

around 520 nm, corresponding to Au_{25} NCs, disappeared (Figure 1C, black line). These observations hint the possible change of the Au_{25} core structure of the BSAGNCs caused by CSH. The effect of the solution pH on the CSH-induced changes in the fluorescence emission of BSAGNCs was measured, and the maximum effect was achieved at pH 8.5, as shown in Figure 1D.

A series of characterizations was carried out towards a better understanding of the possible interactions between the BSAGNCs and CSH. XPS was firstly employed to determine the oxidation states of the NCs before and after reacting with CSH. As for the BSAGNCs, as shown in Figure 2A, the Au $4f_{7/2}$ binding energy (BE) spectrum could be deconvoluted into two components centered at Au(0) BE (83.7 eV) and Au(I) BE (84.4 eV). After reacting with CSH, as shown in Figure 2B, only an enhanced Au(I) peak could be observed at 84.4 eV, indicating full oxidation of Au(0) atoms in the BSAGNCs by CSH. MALDI-TOF-MS was conducted to check the change in the BSAGNCs after reacting with CSH. As the MS spectra indicate, the peak at ~70 kDa (Figure 2C), characteristic of the BSAGNCs (Liu et al., 2010), disappeared after reacting with CSH (Figure 2D). In addition, TEM was used as a complemental tool to characterize the product of the etching reaction. As for the solution of the BSAGNCs, very small NCs could be seen (Figure S1A); however, after reacting with CSH, no clusters could be observed (Figure S1B). These results indicate clearly that the Au core of the BSAGNCs were decomposed owing to the CSH-induced etching process, as schematically illustrated in Scheme 1.

3.3 Interference study

The stability of the BSAGNCs was further examined by using GSH and Cys as etching agent, respectively, both of which have been known to have the etching activity (Chen and Tseng, 2012; Chen et al., 2014a; Shichibu et al., 2007). However, it was found that a large (~1.7 and ~1.4 times) enhancement of red fluorescence emission was observed at room temperature (Figure 3A) after treating of the BSAGNCs with 10 mM GSH and 10 mM Cys at 55 ^{o}C for 1 h, respectively, at pH 8.5. Such enhanced fluorescence ruled out the etching of the BSAGNCs by GSH and Cys, reinforcing the notion of the high stability of the BSAGNCs against thiol etching. GSH and Cys themselves do not exhibit fluorescence. Such enhanced fluorescence could be attributed to direct donation of delocalized electrons of electron-rich atoms or groups of the ligands to the metal core (Wu and Jin, 2010). Since an icosadahedron has 20 triangular faces, the exterior Au_{12} shell is thus incomplete, leaving eight faces uncapped. Perhaps, electron-rich atoms (e.g., N, O) or groups (e.g., -COOH, NH_2) (Wu and Jin, 2010) of GSH and Cys can interact with the Au_{25} surface through these uncapped faces for direct donation of their delocalized electrons to Au_{25}, resulting in the enhanced fluorescence emission. Moreover, as revealed in Figure 3B, low concentration Cys and GSH had a relatively small effect on the fluorescence emission of the BSAGNCs, indicating the concentration-dependent effect, consistent to previous report (Cui et al., 2012). However, as for Cys and GSH, in the presence of CSH, the fluorescence quenching of the BSAGNCs was still observed (see the blue and cyan lines in Figure 3A, and Figure 3B). Such a phenomenon indicates that the presence of GSH and Cys can't stop the etching of the BSAGNCs by CSH. These observations highlight the differences in the stabilities of the BSAGNCs facing different thiols. Although Cys and GSH having free thiol groups have shown the

abilities of chemical etching of noble metal NCs (Chen and Tseng, 2012; Shichibu et al., 2007; Yuan et al., 2013), CSH seems to be a more powerful etchant. Indeed, the etching ability of thiols is associated with their alkyl substituents (Wilcoxon and Provencio, 2003). We also tested the specificity of fluorescence quenching of the BSAGNCs caused by CSH through conducting control experiments using other 19 natural amino acids (nonthiol-containing) as interferences. Owing to the specific thiol-Au interaction, the fluorescent BSAGNCs showed superior selectivity for CSH over them, as shown in Figure 3B.

3.4 Detection of CSH

On the basis of the above results, we then proceeded to develop an etching-based strategy for selective sensing free CSH. Under the optimal pH condition (pH 8.5) as aforementioned, we used the BSAGNCs probe to detect various concentrations of CSH in solution. As shown in Figure 4, the F/F_0 decreased linearly (R^2=0.9969) after increasing the concentration of CSH over the range of 500 nM to 10000 nM. F_0 and F correspond to the fluorescence intensity of the BSAGNCs in the absence and presence of CSH, respectively. The limit of detection (LOD) for CSH was 150 nM (S/N=3). The sensitivity of this method is comparable to most of the previous CSH sensors (Table 1). Moreover, from Table 1, it can also be seen that all of the previous methods for sensing CSH need the extra derivation procedures and/or separation operations, as mentioned above, to obtain the selectivity. The developed method was also applied to the analysis of human serum samples without complicated derivations and separations procedures. A suitable volume of the pretreated solution of blood serum samples was appropriately spiked with the standard solution of CSH and three samples at the same concentration of CSH (6.6 μM) were obtained for analysis. The analysis results

showed that quantitative recoveries of all cases between 98.6 and 101.8% were achieved (Table S1). These results show that this method has potential for quantitative determination of free CSH in human serum samples.

4. Conclusions

In this study, the CSH etching-induced fluorescence quenching of the BSAGNCs has been used to develop an etching-based method for label-free, separation-free, and selective sensing of CSH for the first time. CSH was found to exhibit powerful etching ability. CSH effectively etched the BSA-protected Au NC core, causing the fluorescence quenching. Other thiol-containing species in human blood serum such as Cys and GSH and other 19 natural amino acids did not interfere with the chemical etching by CSH. Under the optimal pH condition (pH 8.5), the linear range between the F/F_0 and the concentrations of CSH was from 500 nM to 10000 nM with a LOD of 150 nM (S/N=3). With the developed method, the deproteined human serum samples spiked with CSH were analyzed with satisfactory results.

Acknowledgements

This work was financially supported by the National Natural Science Foundation of China (Grant No. 21175010 and 21275017), the International Joint Key Project from the Ministry of Science and Technology of China (2010DFB23160), the Fundamental Research Funds for the Central Universities (FRF-BR-11-005A), the Project-sponsored by SRF for ROCS, SEM, and the grant from Beijing Municipal Science and Technology Commission (z131102002813058).

References

Chen, T.-H., Tseng, W.-L., 2012. Small 8, 1912-1919.

Chen, Y., Li, W., Wang, Y., Yang, X., Chen, J., Jiang, Y., Yu, C., Lin, Q., 2014a. J. Mater. Chem. C 2, 4080-4085.

Chen, Y., Li, W.Y., Wang, Y., Yang, X.D., Chen, J., Jiang, Y.N., Yu, C., Lin, Q., 2014b. J. Mater. Chem. C 2, 4080-4085.

Chen, Z., Qian, S., Chen, X., Gao, W., Lin, Y., 2012. Analyst 137, 4356-4361.

Cui, M. L., Liu, J. M., Wang, X. X., Lin, L. P., Jiao, L., Zhang, L. H., Zheng, Z. Y., Lin, S. Q., 2012. Analyst 137, 5346-5351.

Ensafi, A.A., Karimi-Maleh, H., 2010. Electroanalysis 22, 2558-2568.

Gibrat, C., Cicchetti, F., 2011. Prog. Neuropsychopharmacol. Biol. Psychiatry 35, 380-389.

Jin, R., Qian, H., Wu, Z., Zhu, Y., Zhu, M., Mohanty, A., Garg, N., 2010. J. Phys. Chem. Lett. 1, 2903-2910.

Karimi-Maleh, H., Biparva, P., Hatami, M., 2013a. Biosens. Bioelectron. 48, 270-275.

Karimi-Maleh, H., Salimi-Amiri, M., Karimi, F., Khalilzadeh, M.A., Baghayeri, M., 2013b. J. Chem. 2013, 946230.

Kataoka, H., Tanaka, H., Makita, M., 1994. J. Chromatogr. B 657, 9-13.

Kessler, A., Biasibetti, M., Silva Melo, D.A., Wajner, M., Dutra-Filho, C.S., Souza Wyse, A.T., Wannmacher, C.M.D., 2008. Neurochem. Res. 33, 737-744.

Keyvanfard, M., Sami, S., Karimi-Maleh, H., Alizad, K., 2013. J. Brazil. Chem. Soc. 24, 32-39.

Kruusma, J., Benham, A.M., Williams, J.A.G., Kataky, R., 2006. Analyst 131, 459-473.

Kubalczyk, P., Bald, E., 2008. Electrophoresis 29, 3636-3640.

Kusmierek, K., Glowacki, R., Bald, E., 2005. Anal. Bioanal. Chem. 382, 231-233.

Li, G., Jiang, D.E., Kumar, S., Chen, Y.X., Jin, R.C., 2014a. Acs Catal. 4, 2463-2469.

Li, L., Dou, L.G., Zhang, H., 2014b. Nanoscale 6, 3753-3763.

Lin, H., Li, L., Lei, C., Xu, X., Nie, Z., Guo, M., Huang, Y., Yao, S., 2013. Biosens. Bioelectron. 41, 256-261.

Liu, Y., Ai, K., Cheng, X., Huo, L., Lu, L., 2010. Adv. Funct. Mater. 20, 951-956.

Lochman, P., Adam, T., Friedecky, D., Hlidkova, E., Skopkova, Z., 2003. Electrophoresis 24, 1200-1207.

Luo, Z.T., Zheng, K.Y., Xie, J.P., 2014. Chem. Commun. 50, 5143-5155.

Mao, Z.K., Choo, Y.S., Lesort, M., 2006. Eur. J. Neurosci. 23, 1701-1710.

Ogony, J., Mare, S., Wu, W., Ercal, N., 2006. J. Chromatogr. B 843, 57-62.

Ojani, R., Raoof, J.-B., Zarei, E., 2009. Electroanalysis 21, 1189-1193.

Senthamizhan, A., Celebioglu, A., Uyar, T., 2014. J. Mater. Chem. A 2, 12717-12723.

Shiang, Y.-C., Huang, C.-C., Chen, W.-Y., Chen, P.-C., Chang, H.-T., 2012. J. Mater. Chem. 22, 12972-12982.

Shichibu, Y., Negishi, Y., Tsunoyama, H., Kanehara, M., Teranishi, T., Tsukuda, T., 2007. Small 3, 835-839.

Smolin, L.A., Schneider, J.A., 1988. Anal. Biochem. 168, 374-379.

Stachowicz, M., Lehmann, B., Tibi, A., Prognon, P., Daurat, V., Pradeau, D., 1998. J. Pharm. Biomed. Anal. 17, 767-773.

Su, L., Shu, T., Wang, Z., Cheng, J., Xue, F., Li, C., Zhang, X., 2013. Biosens. Bioelectron. 44, 16-20.

Taherkhani, A., Karimi-Maleh, H., Ensafi, A.A., Beitollahi, H., Hosseini, A., Khalilzadeh, M.A., Bagheri, H., 2012. Chinese Chem. Lett. 23, 237-240.

Ueki, I., Stipanuk, M.H., 2009. J. Nutrition 139, 207-214.

Venkatesh, V., Shukla, A., Sivakumar, S., Verma, S., 2014. Acs Appl. Mater. Inter. 6, 2185-2191.

Wen, X., Yu, P., Toh, Y.-R., Tang, J., 2012. J. Phys. Chem. C 116, 11830-11836.

White, P.C., Lawrence, N.S., Davis, J., Compton, R.G., 2002. Electroanalysis 14, 89-98.

Wilcoxon, J.P., Provencio, P., 2003. J. Phys. Chem. B 107, 12949-12957.

Wu, J.F., Sandberg, M., Weber, S.G., 2013. Anal. Chem. 85, 12020-12027.

Wu, Z., Jin, R., 2010. Nano Lett. 10, 2568-2573.

Xie, J., Zheng, Y., Ying, J.Y., 2009. J. Am. Chem. Soc. 131, 888-889.

Xu, Y., Sherwood, J., Qin, Y., Crowley, D., Bonizzoni, M., Bao, Y., 2014. Nanoscale 6, 1515-1524.

Yu, Y., Yao, Q., Luo, Z., Yuan, X., Lee, J.Y., Xie, J., 2013. Nanoscale 5, 4606-4620.

Yuan, X., Tay, Y., Dou, X., Luo, Z., Leong, D.T., Xie, J., 2013. Anal. Chem. 85, 1913-1919.

Scheme 1. Fluorescence quenching of the BSAGNCs caused by CSH-induced etching.

Figure Captions

Figure 1. (A) UV-vis absorption spectrum and fluorescence emission spectrum of the BSAGNCs. Inset: photographs of the BSAGNCs solution under visible light (a) and 365 nm UV light (b). (B) Fluorescence emission spectra of the BSAGNCs solution measured at room temperature before (black line) and after heating at 55 ^{o}C for 1 h (red line). (C) UV-vis absorption spectrum and fluorescence emission spectrum of the BSAGNCs after reacting with 10 mM CSH at 55 ^{o}C. Inset: photographs of the resultant solution under visible light (a) and 365 nm UV light (b). (D) Effect of pH on the CSH-induced fluorescence quenching of the BSAGNCs.

Figure 2. XPS spectra of Au 4f core-level for the BSAGNCs before (A) and after reacting with 10 mM CSH at 55 ^{o}C (B). MAIDL-TOF-MS spectra of the BSAGNCs (C) and the product of the CSH-induced etching of the BSAGNCs (D). Inset: MAIDL-TOF-MS spectrum of BSA molecules.

Figure 3. (A) Fluorescence emission spectra of the BSAGNCs after reacting with 10 mM Cys (red dashed line) and 10 mM GSH (red solid line) at 55 ^{o}C, respectively, followed by reacting with 10 mM CSH at 55 ^{o}C (blue dashed line and cyan solid line). (B) Fluorescence responses (F/F_0) of the BSAGNCs in the presence of 200 μM natural amino acids, GSH and CSH.

Figure 4. Relative fluorescence (F/F_0) of the BSAGNCs as a function of CSH concentration. Inset: The linear detection region for 0.5-10 μM of CSH.

Table 1. Typical CSH sensors published recently.

Thiol property	Labeled	Electron mediators	Separation	Sensing method	LOD (μm)[a]	Thiol selectivity	ref
Etching	NU[b]	NU[b]	NU[b]	**Fluorescence**	**0.15**	**Yes**	**This work**
Nucleophilic	2-Chloro-1-methylquinolinium tetrafluoroborate	NU[b]	HPLC	UV-vis absorption	0.1	Yes	(Kusmierek et al., 2005)
Nucleophilic	N-(1-pyrenyl)maleimide	NU[b]	HPLC	Fluorescence	0.01	Yes	(Ogony et al., 2006)
Nucleophilic	2-Chloro-1-methylquinolinium tetrafluoroborate	NU[b]	CE[d]	UV-vis absorption	0.8	Yes	(Kubalczyk and Bald, 2008)
Reducing	NU[b]	Ferrocyanide	NU[b]	Electrochemical	79.7	No	(Ojani et al., 2009)
Reducing	NU[b]	Aminophenol	NU[b]	Electrochemical	0.14	No	(Ensafi and Karimi-Maleh, 2010)
Reducing	NU[b]	Ferrocene	NU[b]	Electrochemical	0.3	No	(Taherkhani et al., 2012)
Reducing	NU[b]	Ferrocenecarboxaldehyde	NU[b]	Electrochemical	0.06	No	(Karimi-Maleh et al., 2013b)
Reducing	NU[b]	3,4-dihydroxy cinnamic acid	NU[b]	Electrochemical	0.09	No	(Keyvanfard et al., 2013)
Reducing	NU[b]	DEDE[c]	NU[b]	Electrochemical	0.007	No	(Karimi-Maleh et al., 2013a)

[a] LOD: limit of detection; [b] NU: no use; [c] DEDE: (9, 10-dihydro-9, 10-ethanoanthracene-11, 12-dicarboximido)-4-ethylbenzene-1, 2-diol; [d] CE: capillary electrophoresis.

Highlights

- Cysteamine is a strong etchant.
- Cysteamine can selectively quench the fluorescence emission of the BSA-protected Au_{25} nanoclusters in the presence of glutathione and cysteine.
- An etching-based, label-free and separation-free fluorescent method is developed for selectively sensing cysteamine.
- The detection limit for cysteamine is 150 nM (S/N=3).

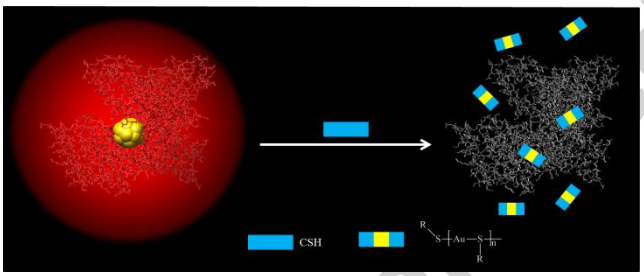

Scheme 1.

Figure 1 – Su, L. *et al*

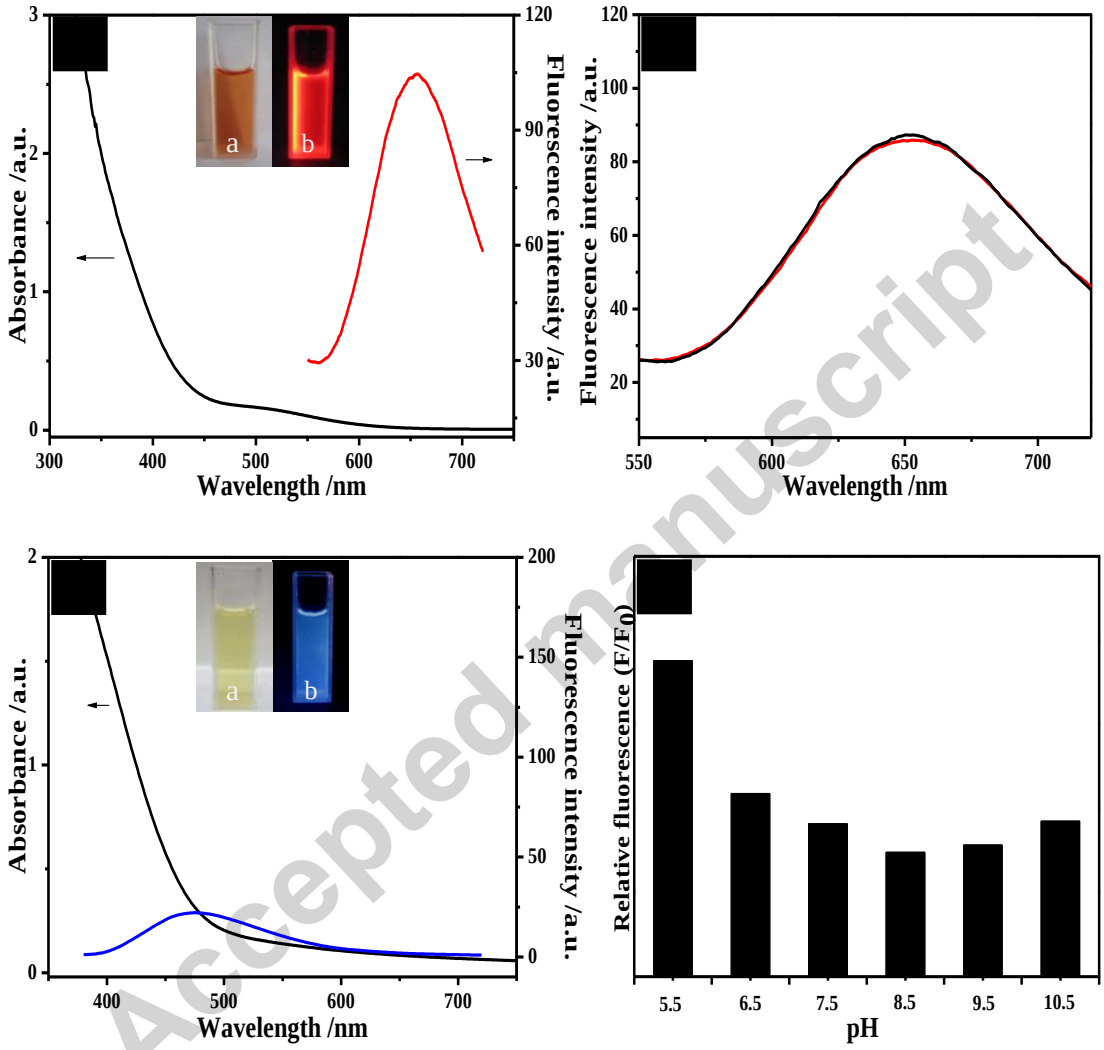

Figure 2 – Su, L. *et al*

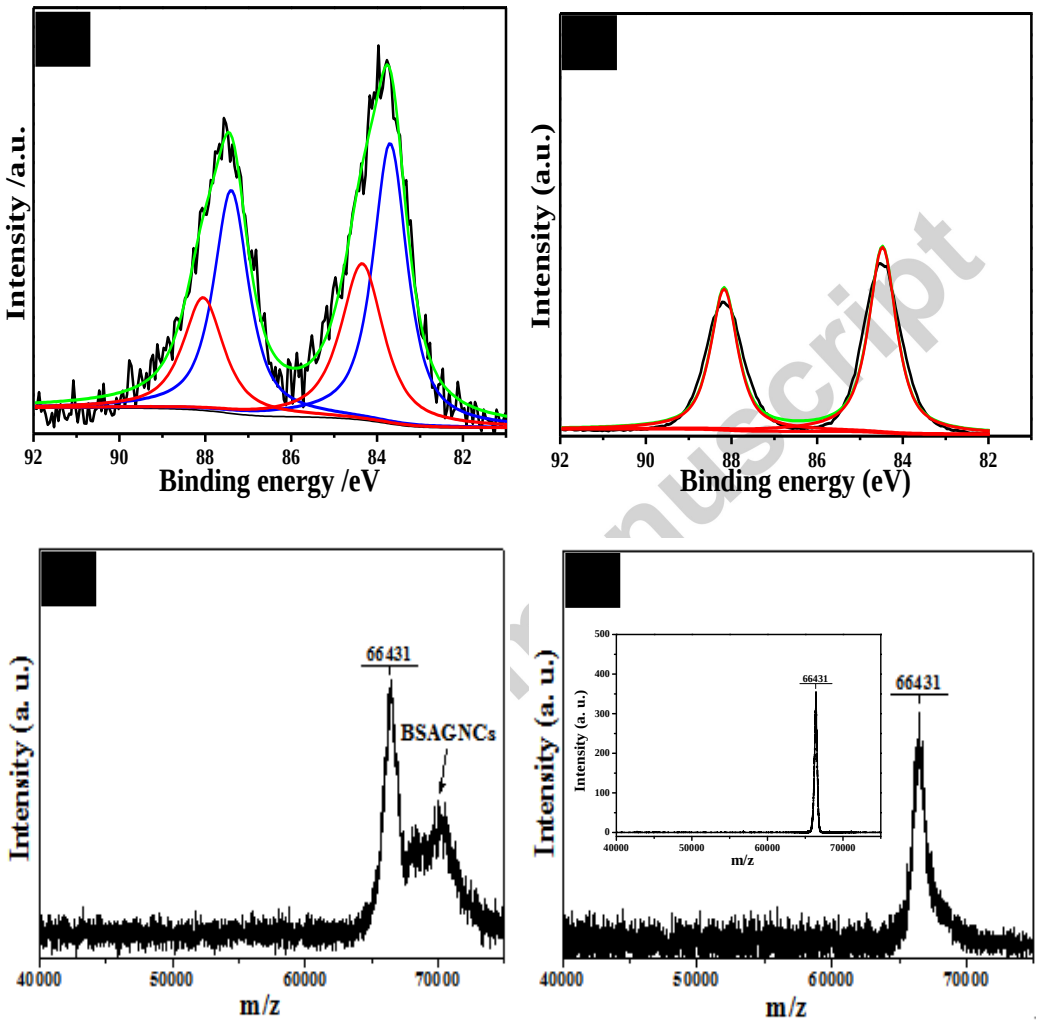

Figure 3 – Su, L. *et al*

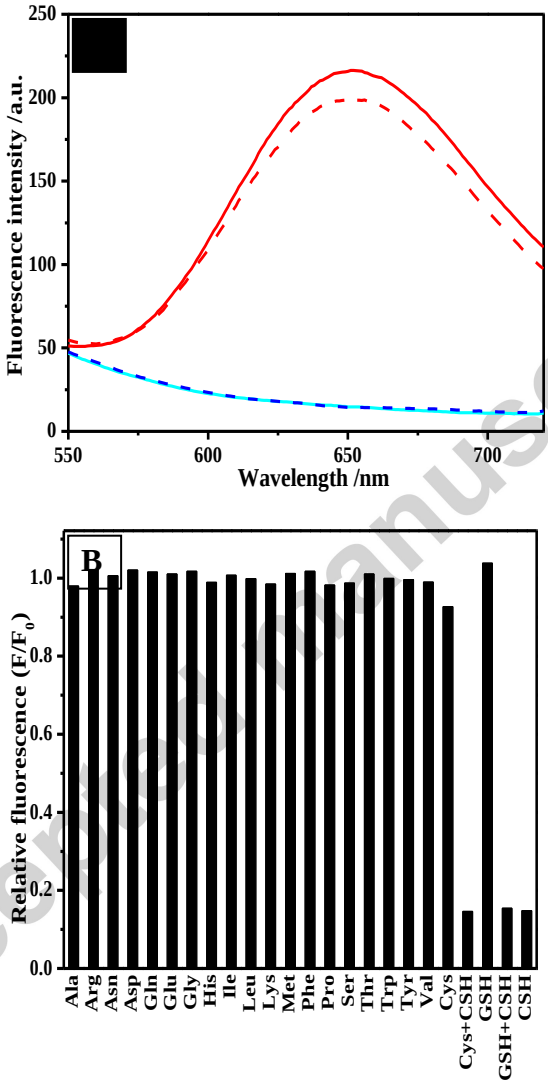

Figure 4 – Su, L. *et al*